Equilibrium Topology of the Intermediate State in Type-I Superconductors of Different Shapes

Ruslan Prozorov*

Ames Laboratory and Department of Physics & Astronomy, Iowa State University, Ames, Iowa 50011, USA

A high-resolution magneto-optical technique was used to analyze flux patterns in the intermediate state of bulk Pb samples of various shapes—cones, hemispheres, and discs. Combined with the measurements of macroscopic magnetization, these results allowed studying the effect of bulk pinning and geometric barrier on the equilibrium structure of the intermediate state. Zero-bulk pinning discs and slabs show hysteretic behavior due to topological hysteresis—flux tubes on penetration and lamellae on flux exit. (Hemi)spheres and cones do not have a geometric barrier and show no hysteresis with flux tubes dominating the intermediate field region in both regimes. It is concluded that flux tubes represent the equilibrium topology of the intermediate state. Real-time video is available in the EPAPS Document No. E-PRLTAO-98-024726..

Pattern formation in strongly correlated systems is a topic of incessant interest for a broad scientific community [1]. At first sight, type-I superconductors represent a perfect physical system where it is relatively easy to tune the parameters and try to understand the physics behind the observed topology of the intermediate state. In fact, analogies to type-I superconductors extend from astrophysics [2] to the physics of ice [3]. The fundamental problem, however, is that in a finite system, it is impossible to predict a 2D and moreover 3D pattern based solely on the energy minimization arguments [4]. The pattern has to be assumed, and then its geometrical parameters are determined from the minimization. Back in the 1930s, Lev Landau suggested a simple stripe model, which was possible to analyze analytically [5,6]. Later refinements (such as domain widening and/or branching) tried to address apparent inconsistencies between the model and the experiment [7–9]. Still, a comprehensive description has never been achieved, with the main problem being multiple observations of the closed-topology structures (flux tubes) in best samples. Experimental and theoretical effort is growing to obtain a general understanding of the problem [4,10–12]. Here, we outline several factors that influence and often determine the topology of the intermediate state and must be taken into account by a successful theory.

The first issue is (bulk) flux pinning. In the overwhelming majority of published papers, this question is simply omitted. We have shown that tubular topology is fairly robust but is destroyed and transformed into a laminar pattern by the structural defects. In more disordered samples with significant bulk pinning, a nonequilibrium dendrite-like topology of the intermediate state is observed [13]. Recently, it was shown that close to H_c, laminar structure transforms into tubular upon applying a small-amplitude ac field to shake it out of the metastable state [14]. Fortunately, it is easy to distinguish between pinning-induced and topological hysteresis. The former becomes larger at the lower fields and reaches maximum at $H = 0$.

The latter is maximal around $H = H_c(1 - N)$ (where N is the demagnetization factor) and should vanish in the limit of $H = 0$. We note that a concept of topological hysteresis as applied to type-I superconductors was introduced to describe the irreversibility in a *macroscopic* response due to different topologies of the intermediate state, e.g., sample magnetic moment [13]. It was later used to describe a subtle specific issue of a crossover between tubes and laminae in films near the H_c [15].

The second crucial ingredient to understand the intermediate state is sample shape and geometry. Films are relatively easy to make and work with, but they provide only very limited experimental information and are at the borderline of applicability of most theories. The effective penetration depth depends on film thickness and, in case of Pb, the sample exhibits behavior of a type-II superconductor below about 0.1 μm [9]. The phase transition in the vicinity of H_c is modified compared to the bulk case [16] and a huge demagnetization factor causes any small defects on the film edge to act as centers of premature flux penetration. In addition, the geometric barrier [17] plays a dominant role and actually determines the flux pattern [18]. On the other hand, experiments with thick pinning-free type-I superconducting slabs and disks have consistently showed the tubular pattern upon flux penetration and laminar structure pattern upon flux exit. It was directly observed in single crystals of Sn back in 1958 [19], Hg , and Pb [8,20]. The tubular pattern was reproduced numerically [21] and metastability of slabs was theoretically analyzed [22]. Ginzburg-Landau equations have stable multiquanta solution for arbitrary tube size [9]. Still, the unsatisfactory fact is that in any shape where there are two parallel surfaces perpendicular to the magnetic field, there will be a geometric barrier that promotes an edge instability and drives the tubes into the interior [7]. The barrier was different for the flux exit; therefore, tubes were considered to be a result of the metastable state determined by the geometric barrier.

In this Letter, we study *pinning-free* samples of various shapes—discs, (hemi) spheres, and cones. The latter two geometries do not have the geometric barrier (as directly proven by the observations), yet show that flux tubes exist both upon flux entry and exit proving that flux tubes represent the equilibrium topology of type-I superconductors.

Quantum design Magnetic Property Measurement System (MPMS) magnetometer was used for magnetization measurements. Magneto-optical (MO) imaging was performed in a pumped flow-type optical ^{4}He cryostat using Faraday rotation of a polarized light in Bi—doped iron-garnet films with in-plane magnetization [13]. In all images, bright regions correspond to the normal state and dark regions to the superconducting state. Because of a very large volume of images and video, we could only include a small subset of data in this Letter. For complete coverage, including real-time video, see Ref. [20].

We begin with a single crystal of lead in the form of a disk of diameter $d = 5$ mm and thickness $t = 1$ mm. Four crystals of different orientations, (110) and (100), and from different companies, *MaTecK GmbH* and *Metal Crystals and Oxides Ltd.*, were studied. The *MaTecK* crystals showed lowest residual magnetic hysteresis and correspondingly clearer patterns of the intermediate state. Figure 1 shows magnetization loop measured in a (100)-oriented Pb single crystal at $T = 4.5$ K. The hysteresis vanishes at $H \rightarrow 0$, and minor hysteresis loops (shown by smaller open symbols with the field sweep direction indicated by arrows) show no hysteresis. Larger open symbols show the result of a field-cooling experiment. They coincide with the data obtained by sweeping the magnetic field down. These observations imply zero-bulk pinning, and we assert that the hysteresis comes from the difference

in topologies of the intermediate state upon flux entry and exit.

This assertion is directly confirmed by the magneto-optical images shown in Fig. 2. The left column shows flux penetration, the right column—flux exit. There is obvious difference between the topologies of the flux patterns. The tubes have sizes from μm at low fields to submm at higher fields. We note that tubular structure is only observable in samples with no pinning (pinning leads to dendrites [13]). Online video figures also show robustness of the flux tubes upon penetration of a tilted field [20]. It is important to note that although laminar structure appears on a hysteretic branch, it matches the field-cooled data indicating that this irreversibility is not due to macroscopic flux gradient and cannot be "quenched" by the annealing. We also note that tubular pattern appears on an ascending branch that behaves as a textbook $M(H)$ loop, providing additional evidence for its equilibrium state.

In fact, observation of a closed topology on flux entry and open on flux exit is quite typical for any sample with two flat surfaces perpendicular to the applied field. The

FIG. 1 (color online). $M(H)$ loop measured in a Pb single crystal at $T = 4.5$ K. Larger open symbols show measurements each after field cooling at indicated field to 4.5 K. Small open symbols show minor hysteresis loops.
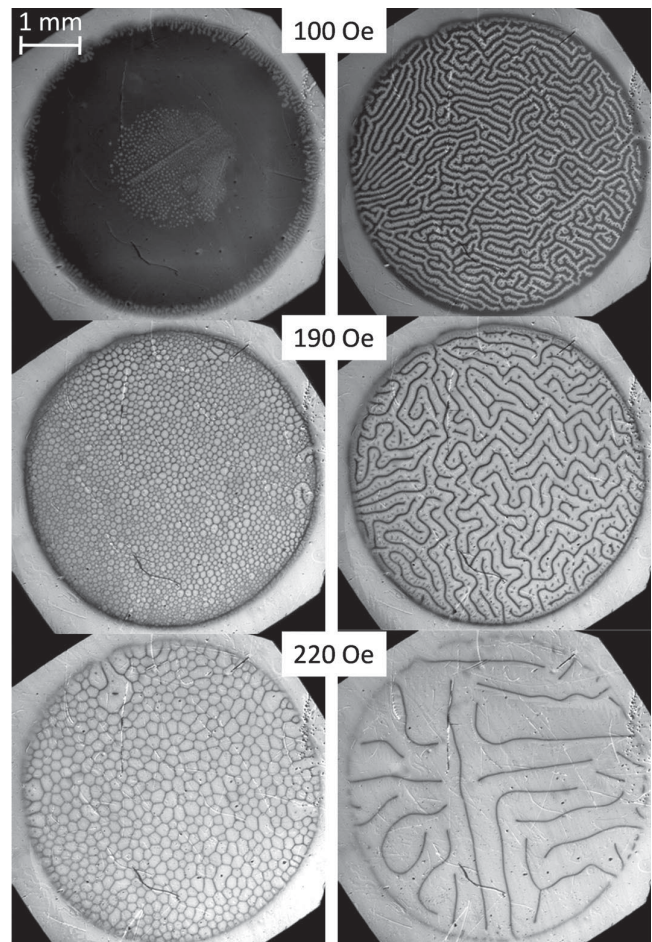
FIG. 2. Structure of the intermediate state in a disc-shaped Pb single crystal at 5 K. Left column—increasing magnetic field after ZFC. Right column—decreasing field.
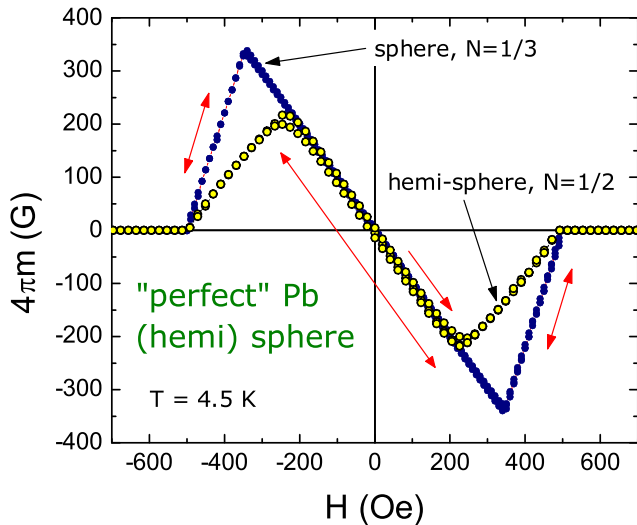
FIG. 3 (color online). Magnetization loop in a "perfect super-conducting" sphere (solid symbols) and a hemisphere (open symbols) at $T = 4.5$ K.

flux structure is governed by the geometric barrier [17]. When a magnetic field is increased, Meissner currents flow on both surfaces even in a thick disc [23]. Any closed-flux object will be instantaneously driven to the sample center by the Lorentz force. Therefore, it will appear as if the flux tubes pile up from the center outwards, exactly as it is observed in Fig. 2. To eliminate the geometric barrier, the sample should be in the form of an ellipsoid. In that case, the Lorentz force is *exactly* balanced by the condensation energy force upon flux penetration. A comprehensive study of the shape effect on magnetic hysteresis was reported in Ref. [24] where the authors arrived at a clear conclusion that shape plays an important role and showed that ellipsoidal sample has no hysteresis. Figure 3 shows experimentally such "perfect" $M(H)$ loops measured in a Pb sphere (solid symbols) and a hemisphere (open symbols). The sphere was produced by dropping molten lead (99.9999% pure) in an inert atmosphere. The hemisphere was cast into a copper mould in an inert atmosphere and subsequently polished and annealed in vacuum at 250 °C for 24 hours. Still, the surface was not perfect, and defects are seen in the imaging. Figure 4 shows the results for a hemisphere. (Inset shows another hemisphere sample.) The major result is evident—the geometric barrier is no longer present (no domelike formation of flux in the center) and flux tubes appear *both* ways—on flux entry and flux exit. Real-time video of another hemisphere is available at [20].

The video also shows flux tubes formation upon field cooling as well as warming up from the pure Meissner state. Therefore, in a hemisphere, flux tubes appear from all four possible ways to reach a particular point inside the intermediate state domain on an H-T phase diagram.

Another shape where the geometric barrier is not present is a cone. The cones are interesting because one can go from an obtuse to an acute cone, and quite possibly the
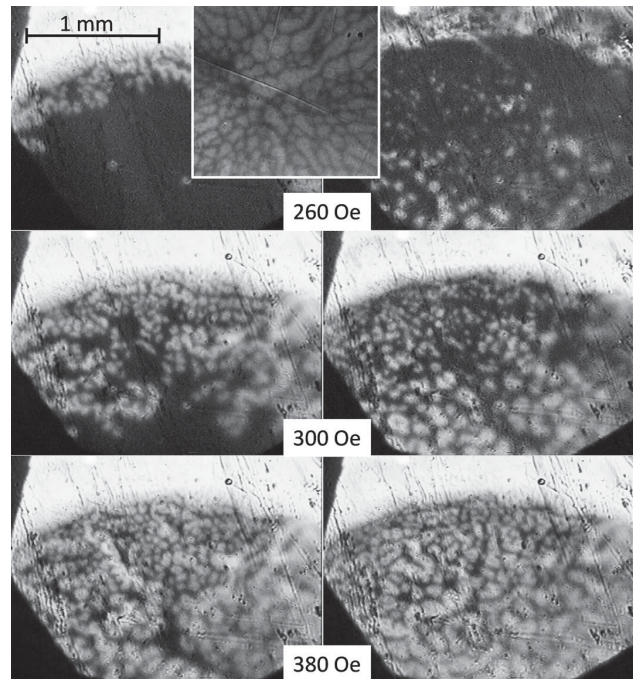
FIG. 4. Flux penetration (left column) and exit (right column) in a Pb hemisphere ($d = 4$ mm) at $T = 4$ K and indicated magnetic fields. Inset shows tubular pattern in a different hemisphere sample.

topology of the intermediate state will change. However, it is very difficult to produce stress-free samples. We report data on the obtuse cone (4 mm diameter, 1 mm height) in Fig. 5. The rounded shape of the curve is apparently due to large local demagnetization at the corners. Overall, the curve is quite reversible.

Figure 6 shows magneto-optical imaging obtained in a conical sample. Despite the presence of some defects and
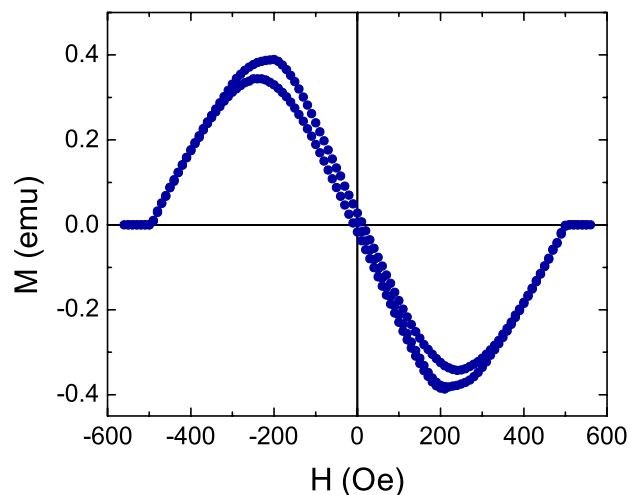
FIG. 5 (color online). Magnetization loop in a cone at $T = 4.5$ K.
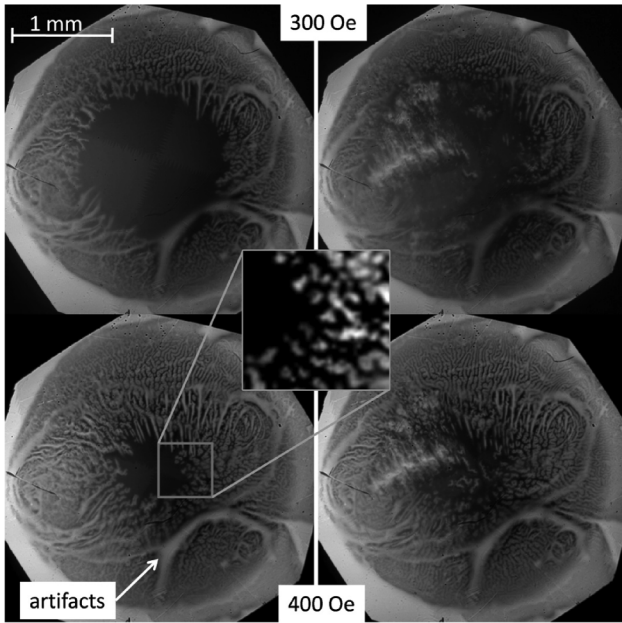
FIG. 6.   Flux penetration (left column) and exit (right column) into a cone-shaped sample at 4 K and at indicated fields. Inset shows a zoom of the tubular pattern.

artifacts (from grease and surface imperfections), there is a clear absence of the geometric barrier and presence of flux tubes.

We conclude that a tubular structure appears to be the equilibrium topology of the intermediate state because it is always observed on flux penetration in samples of any shape, as well as on flux exit and upon warming and cooling in constant field in samples without geometric barrier. Laminar structure, on the other hand, is unstable in the presence of force—either Lorentz or condensation energy. In flat samples, geometric barrier is present on penetration, but not on exit. In this case, the laminar structure is formed as flux-percolative state at high fields, which breaks into tubes at smaller fields (as was foreseen by Landau [6]). In samples without geometric barrier, there is always a condensation energy gradient that destroys the laminar pattern. Our more recent experiments also show transformation of the laminar pattern into tubular by applied external current. Importantly, our observations emphasize that different topologies result in actual macroscopic (topological) hysteresis in magnetization as evident from Fig. 1.

I thank Jacob Hoberg and Baozhen Chen for help with the experiments. Discussions with John Clem, Kotane Dam, Rudolf Huebener, Vladimir Kogan, and Roman Mints are greatly appreciated. Ames Laboratory is oper-

---

*prozorov@ameslab.gov

 [1] D. Walgraef, *Spatio-Temporal Pattern Formation* (Springer, Ney York, 1997).
 [2] K. B. W. Buckley, M. A. Metlitski, and A. R. Zhitnitsky, Phys. Rev. Lett. **92**, 151102 (2004).
 [3] R. Wang *et al.*, Phys. Rev. Lett. **97**, 167802 (2006).
 [4] R. Choksi, R. V. Kohn, and F. Otto, J. Nonlinear Sci. **14**, 119 (2004).
 [5] L. D. Landau, Sov. Phys. JETP **7**, 371 (1937); L. Landau, Nature (London) **141**, 688 (1938).
 [6] L. D. Landau, J. Phys. (Moscow) **7**, 99 (1943).
 [7] J. D. Livingston and W. DeSorbo, in *Superconductivity*, edited by R. D. Parks (Marcel Dekker, Inc., New York, 1969), Vol. 2, p. 1235.
 [8] R. P. Huebener, *Magnetic Flux Structures of Superconductors* (Springer-Verlag, New-York, 2001).
 [9] M. Tinkham, *Introduction to Superconductivity* (Dover Books on Physics, New York, 2004).
[10] F. Liu, M. Mondelo, and N. Goldenfeld, Phys. Rev. Lett. **66**, 3071 (1991).
[11] R. E. Goldstein, D. P. Jackson, and A. T. Dorsey, Phys. Rev. Lett. **76**, 3818 (1996).
[12] A. T. Dorsey and R. E. Goldstein, Phys. Rev. B **57**, 3058 (1998).
[13] R. Prozorov *et al.*, Phys. Rev. B **72**, 212508 (2005).
[14] M. Menghini and R. J. Wijngaarden, Phys. Rev. B **75**, 014529 (2007).
[15] C. Gourdon, V. Jeudy, and A. Cebers, Phys. Rev. Lett. **96**, 087002 (2006).
[16] L. M. Abreu, and A. P. C. Malbouisson, Phys. Lett. A **322**, 111 (2004).
[17] E. Zeldov *et al.*, Phys. Rev. Lett. **73**, 1428 (1994).
[18] H. Castro *et al.*, Phys. Rev. B **59**, 596 (1999).
[19] A. L. Schawlow and G. E. Devlin, Phys. Rev. **110**, 1011 (1958).
[20] See EPAPS Document No. E-PRLTAO-98-024726 for real-time videos. http://www.cmpgroup.ameslab.gov/ supermaglab/video/Pb.html. For more information on EPAPS, see http://www.aip.org/pubservs/epaps.html.
[21] H. Bokil and O. Narayan, Phys. Rev. B **56**, 11195 (1997).
[22] A. Fortini, A. Hairie, and E. Paumier, Phys. Rev. B **21**, 5065 (1980).
[23] R. Prozorov *et al.*, Phys. Rev. B **62**, 115 (2000).
[24] J. Provost, E. Paumier, and A. Fortini, J. Phys. F **4**, 439 (1974).